Lightweight and strong gelling agent-reinforced injection-molded polypropylene composite foams fabricated using low-pressure CO_2 as the foaming agent

Qian Ren[1,2,+], Minghui Wu[1,+], Zhengsheng Weng[1,3], Long Wang[1,2,*], Wenge Zheng[1,2,*], Yuta Hikima[4], Masahiro Ohshima[4,*]

[1]*Ningbo Key Lab of Polymer Materials, Ningbo Institute of Material Technology and Engineering, Chinese Academy of Sciences, Ningbo, 315201, China*

[2]*University of Chinese Academy of Sciences, Beijing, 100049, China*

[3]*Faculty of Materials Metallurgy and Chemistry, Jiangxi University of Science and Technology, Ganzhou, 341000, China*

[4]*Department of Chemical Engineering, Kyoto University, Katsura, Kyoto 6158510, Japan*

[+] These authors contributed equally to this work.

ABSTRACT: Lightweight and strong polymeric foams show high potential application in alleviating the global energy crisis due to their capability of reducing material and resource requirements as well as decreasing energy consumption. However, it is inevitably difficult to produce lightweight polymers with satisfactory mechanical properties. Herein, we report an innovative method to produce high-performance polypropylene (PP) foams by combining a sorbitol gelling agent with the newly developed low-pressure microcellular injection molding (MIM) technique. Carbon dioxide (CO_2) at an ultralow pressure of 5 MPa is used as a foaming agent in the low-pressure MIM process. The addition of a 1,3:2,4-bis-O-(4-methyl benzylidene)-D-sorbitol gelling agent (MDBS), which generates an in situ network structure, notably enhances

the crystallization, viscoelasticity and melt strength of PP, resulting in PP foams with well-defined cellular structures. Compared with neat PP foams, the added sorbitol gelling agent leads to a four orders of magnitude increase in the cell density of PP foams that have a cell size of approximately 8.4 μm. Remarkably, the tensile toughness and tensile strength of the PP composite foam are approximately 1000% and 150% higher than those of the neat PP foam, respectively. These results demonstrate that lightweight and strong PP foams with high ductility can be obtained via the scalable and novel FIM technique, which shows a promising future in many applications, such as automotive, construction and electrical components.

Keywords: Polypropylene, Gelling agent, Carbon dioxide, Microcellular foam, Mechanical properties

1. INTRODUCTION

Microcellular injection molding (MIM) is an advanced and efficient green foaming method that utilizes either nitrogen or carbon dioxide as a physical blowing agent to fabricate foamed products with complex, three-dimensional structures [1, 2]. In contrast to the conventional structural foam injection molding process that uses chemical blowing agents as the foaming agent, MIM yields foamed parts with much smaller cell sizes and higher cell densities, thus producing foams with very good mechanical properties [3−5]. As a result, many researchers have conducted MIM with different polymers, including polypropylene (PP) [5−9], polyamide 6 (PA6) [10], and polylactide (PLA) [11,12]. Moreover, compared with traditional solid injection molding technology, MIM yields foamed parts with less material consumption and residual stress, fewer

molding cycles, and higher dimensional stability [3]. Furthermore, the microcellular injection-molded foams produced with MIM usually exhibit much higher toughness and better acoustic and thermal insulation than solid injection-molded samples [12–14]. Despite these advantages, the wide commercial application of MIM technology has not been realized. One of the representative MIM technologies is MuCell® injection molding technology, which consists of a pressurized system for the supercritical fluid (SCF) and a specifically configured screw for the melt polymer [6,7]. In a typical MuCell® injection molding process, an expensive SCF pumping system is a must to pressurize N_2 or CO_2 to 15–40 MPa, which inevitably increases the operation and machine costs. Therefore, the industrial application of MIM technology is very low.

Recently, we developed a novel FIM system entitled resilient and innovative cellular foam injection molding (RIC-FIM), which demonstrates that the traditional process of pressurizing gas such as N_2 or CO_2 to very high pressure for the regular MIM process can be removed with this ingenious design [15,16]. In this RIC-FIM technology, a low-pressure gas is directly provided from a regular gas cylinder and injected into the screw via a delivery hole and a pressure vessel. Unlike the use of a gas at 15–40 MPa in the MuCell FIM process, low gas pressures, such as 5–8 MPa of N_2 or CO_2, could be used as physical blowing agents and can produce injection-molded parts with a fine cellular structure and favorable void fraction [17,18]. Additionally, we demonstrated that low-pressure air could also be used as a novel foaming agent to produce injection-molded PP foams; interestingly, the melt properties and molecular structures of PP were simultaneously modified, acting as a reactive foaming process [19]. However, it is still a challenge to produce polymeric foams with favorable mechanical properties and fine cellular structures.

Polymeric foams are a kind of material that has been an increasing focus of studies not only in academia but also in industry [20–23]. Unlike their solid counterparts, microcellular foams

exhibit many merits, including good energy absorption, high impact strength, acoustic and thermal insulation, material conservation, and adjustable mechanical properties [3,24]. Thus, polymeric foams are attractive for many industries, including the automotive, packaging, sporting, cushioning, building, and aerospace industries [3,25]. A wide variety of thermoplastic polymeric foams are available, among which polystyrene (PS) and polyethylene (PE) foams are the most commonly used. However, their low mechanical strength restricts their wide application. As a competitive candidate, polypropylene (PP) can overcome the lower strength of PE and the lower impact strength of PS. Additionally, PP foams exhibit higher thermal stability than PS and PE foams, making them more attractive in the foaming industry. Despite the abovementioned advantages, unmodified PP suffers from several disadvantages, such as its weak melt strength and narrow processing window, resulting in serious cell coalescence and nonuniform cellular structures together with inferior mechanical performance, inevitably limiting its use [4,26]. To address these problems that arise from the poor melt strength of PP, various approaches, including polymer blending [5,27], chemical crosslinking, the introduction of long-chain branching [28−30], and the addition of various particles and fibers [31−34], have been proposed to modify PP to obtain a suitable melt strength, desirable crystallization properties, and attractive foaming performance.

The addition of nanoparticles is an efficient and viable method to endow polymeric materials with fine cellular structures and favorable mechanical properties [35−38]. Several studies have revealed that the incorporation of nanoparticles can act in the foaming process as a cell nucleating agent due to their high specific surface areas and large aspect ratios, rendering a low energy barrier for cell nucleation [31,32]. Moreover, the incorporation of nanoparticles not only enhances the melt strength of polymers but also improves the crystal nucleation and overall crystallization rate of semicrystalline polymers, which are both critical in the foaming process and endow foams with

the desired cellular structures and mechanical properties [6,7]. Generally, inorganic nanofillers, including nanoclay [32,33], carbon nanotubes [8, 39], and carbon nanofibers [40,41], as well as organic nanofillers such as cellulose nanofibers (CNFs) [6,7,41], have been reported in the microcellular polymer foaming process by using supercritical fluids as physical blowing agents. Moreover, compared with other modification approaches, the addition of nanoparticles can produce extra advantages, such as a high mechanical strength, favorable conductivity, and good electromagnetic shielding properties [42–47], which are dependent on the nature of various nanoparticles. Recently, reports have demonstrated that the in situ fibrillation approach of a second-phase polymer based on polymer blending can effectively enhance the foaming ability of semicrystalline polymers [9,48]. It was revealed that the in situ fibrils/nanofibrils could act as flexible fibers in their network structure, notably enhancing their melt strength, especially the strain-hardening behavior [5,49]. However, they could not enhance the crystallization of semicrystalline polymers, such as PP and PLA, which was similar to the use of inorganic nanofillers. The preparation of in situ fibrillation of a second-phase polymer based on polymer blending is time-consuming and not easily scalable. Careful control of the processing temperature and an elaborate selection of polymer blends with an appropriate difference in their melting temperatures are always needed.

Dibenzylidene sorbitol (DBS) derivatives, which are small-molecule gelators, have shown outstanding properties as crystal nucleators for PP [50–52]. This result is mainly because DBS can in situ form a self-assembled ramified nanofibril at a higher temperature than the crystallization temperature of PP, leading to the formation of a three-dimensional network structure with a large specific area during its cooling process [53]. As a result, these self-assembled ramified nanofibrils can drastically improve the crystallization property of PP and produce PP products with extremely

high transparency. To the best of our knowledge, there is little research on using sorbitol gelling agents to improve the foaming ability of PP. Miyamoto et al. used a sorbitol gelling agent to enhance the foaming property of isotactic PP in the MuCell® FIM process, and open-cell PP foams with nanofibrillated structures were prepared [54]. Later, Wang et al. reported the preparation of fine cells with cell sizes of approximately 2.5 μm and cell densities of over 10^{10} cells/cm^3 by combining the sorbitol gelling agent and MuCell® FIM process [55]. However, the mechanical properties of polymeric foams prepared using RIC-FIM have not yet been studied, while the mechanical performance should be considered when applying the foams to injection-molded parts.

In this work, a new approach that combines a sorbitol gelling agent with a network structure and long-chain branches is developed to prepare strong and supertough PP foams via the newly developed green RIC-FIM technology. CO_2 at a pressure as low as 5 MPa is used as a physical blowing agent. First, the effects of the sorbitol gelling agent on the thermal properties and rheological behavior of PP are investigated. Then, the cellular structures of the injection-molded foams with and without the sorbitol gelling agent are studied. Finally, the influence of the sorbitol gelling agent and the operating conditions of the foaming process on the mechanical properties of the prepared foams are systematically compared.

2. EXPERIMENTAL SECTION

2.1. Materials

A commercially available metallocene-based PP, WAYMAX, MFX3, supplied by the Japan Polypropylene Corporation, Tokyo, Japan, was used as a base polymer. It is a branched PP specially developed for the foaming process. The melt flow rate (MFR) was 8.0 g/10 min (230 °C, 21.6 N), and its density was 0.9 g/cm^3. To enhance the foaming ability of PP, a sorbitol gelling

agent was added to PP. The sorbitol gelling agent used here was a 1,3:2,4-bis-O-(4-methyl benzylidene)-D-sorbitol gelling agent (MDBS) provided by New Japan Chemical [8]. A master batch of PP with 3 wt% MDBS was compounded and kindly provided by the same company. Moreover, 99% pure CO_2, purchased from the Izumi Sangyo, Tokyo, Japan, was used as a physical foaming agent for our foam injection molding experiments.

2.2. Preparation of the Foams

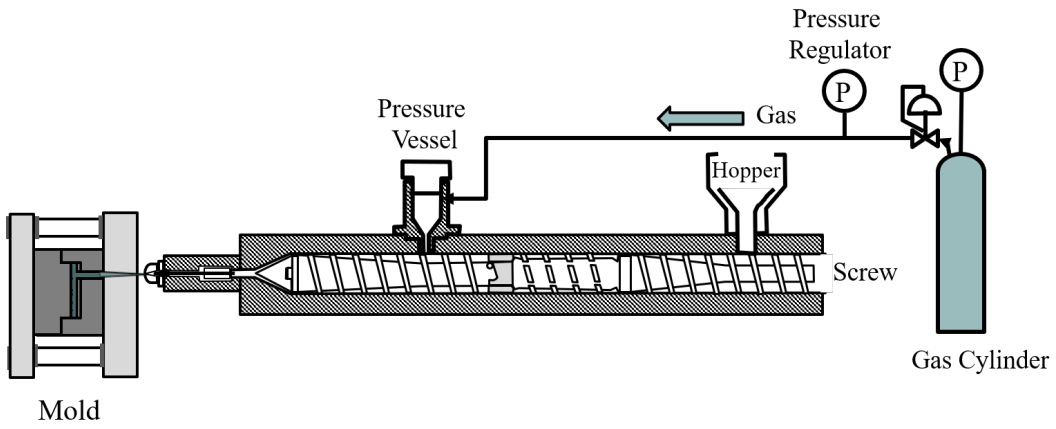

Figure 1. Schematic diagram of the developed resilient and innovative cellular foam injection molding (RIC-FIM) machine.

A 35-ton electric injection molding machine with a 22-mm diameter screw, model J35AD-AD30H, manufactured by Japan Steel Work, Ltd. Hiroshima, Japan, was used to produce the injection molding experiments. Unlike a regular foam injection machine equipped with a MuCell SCF delivery system, there is no supercritical pumping system or injector valve in the RIC-FIM machine, which is schematically depicted in Figure 1. In this novel design, the low-pressure gas acting as the blowing agent can be directly introduced into the molten polymer through a delivery

hole supplied from the gas cylinder, which was described in our earlier work and will not be reiterated here [18,19].

Table 1. Main processing variables used in the foam injection molding process.

Processing Variables	Values
Melt temperature (°C)	190
Injection speed (mm/s)	100
Injection pressure (MPa)	160
Dwelling time (s)	3.0–4.2
Foaming temperature (°C)	86, 91, 97
Core-back rate (mm/s)	20
Core-back distance (mm)	1
CO_2 pressure (MPa)	5
Mold temperature (°C)	40
Shot size (mm)	33
Packing pressure (MPa)	30

Table 1 lists the main processing variables used in the FIM process. CO_2, which has a higher solubility than N_2 in PP, was used as the physical blowing agent, and the gas pressure was as low as 5 MPa. In regular foam injection molding, a high pressure of N_2 is always used as the physical blowing agent [6–8]. A mold used for fabricating the injection-molded foams consisted of a rectangular cavity (70 mm × 50 mm × 2 mm) and a fan gate. To focus the effect of the addition of MDBS on the cellular structure and the mechanical properties of PP foams, the void fraction was set at 50%, which was achieved by performing FIM experiments with a mold-opening (core-back) operation. Consequently, a 50% void fraction or 2-fold expansion of PP foams was produced by shifting a portion of the moveable part of the mold from 0 to 2 mm [4,40]. The final MDBS concentration used here was 0.5 wt%, according to previous results. Hereafter, PP foams with 0.5 wt% MDBS and without MDBS were denoted PP-0.5 and PP-0, respectively. Additionally, to monitor the foaming behavior, two pressure sensors and two temperature sensors were equipped

in the mold cavity, which could perform online monitoring of the pressure and temperature of the polymer in the mold cavity by a data device, Mold Marshaling system EPD-001, Futaba, Chiba-ken, Japan [13,14]. The foaming temperature was defined as the polymer temperature in the cavity at the time that the mold opening operation was initiated [4,54].

2.3. Testing and Characterization

2.3.1. Dynamic rheological measurement

The rheological test was carried out on a stress-controlled ARES dynamic rheometer (TA Instruments, USA) using a parallel plate geometry with a diameter of 25 mm. Before measurement, disk-shaped PP samples with a thickness of approximately 1.0 mm and a diameter of 25 mm were compression molded at 190 °C for 5 min in a hot press. Oscillatory frequency measurements were performed at 190 °C at frequencies ranging from 0.01 to 100 rad/s at a strain of 1%, which was within the linear viscoelasticity regime.

2.3.2. Differential scanning calorimetry measurement

The effect of MDBS on the nonisothermal crystallization behavior of PP was studied using differential scanning calorimetry on a DSC 7020 instrument provided by Hitachi High-Tech Science Corporation, Tokyo, Japan. The tests were conducted with an approximately 5–7 mg specimen under a nitrogen purge. In the nonisothermal crystallization measurements, the specimens were first heated from 30 to 230 °C at a heating rate of 10 °C/min and held for 5 min to eliminate the thermal histories. Subsequently, the specimens were cooled to 30 °C at a designated cooling rate in the range from 2 to 20 °C/min. Finally, the specimens were reheated to

$X_c(\%) = \Delta H_m / \Delta H_m^0 \omega_{pp} \times 100\%$, where ΔH_m , ω_{pp}, and ΔH_m^0 are the melting enthalpy, the mass fraction of PP, and the theoretical heat of fusion of 100% crystalline PP, respectively. A value of 207 J/g was used for the standard heat of fusion of the α-phase of PP [34]. At least three specimens were measured, and the average values were reported.

2.3.3. Foam characterization

To examine the cellular structure of the prepared foams, a Mighty-8 scanning electron microscope (SEM), manufactured by Technex Lab Co., Ltd., Japan, was used. To prepare the SEM specimen, a small piece was cut from the central area of the injection-molded bars. Then, the piece was cryogenically fractured after immersion in liquid nitrogen for approximately 30 min. Afterward, the smoothly fractured surfaces were sputter-coated with a thin layer of gold using a VPS-020 Quick Coater (ULVAC KIKO, Ltd., Japan) for SEM observation. After coating, the prepared specimens were observed by Ting-SEM at an accelerating voltage of 17 kV.

SEM micrographs were analyzed using ImageJ software, provided by the National Institutes of Health, USA, to quantitatively characterize the cellular structures. The average cell size (*d*) of the foams was calculated using the following equation:

$$d = \frac{\sum d_i n_i}{\sum n_i} \quad (1)$$

where n_i is the number of cells with a diameter of d_i, assuming that the cell shape is spherical, and more than two hundred cells were calculated along with the standard deviation. Then, the cell

density (N_0) was obtained as the number of cells per cubic centimeter using the following equation [11]:

$$N_0 = (\frac{n}{A})^{1.5} \quad (2)$$

where n is the number of cells in the selected SEM micrograph, and A is the image area.

2.3.4. Mechanical property testing

Following ISO standard 37-4, tensile measurements were performed at room temperature on an Autograph universal testing instrument (model AGS-1 kN, Shimadzu, Japan) with a gauge length of 12 mm and a crosshead speed of 10 mm/min. The testing samples were cut from the center of the injection-molded bars. Before measurement, all the foams were placed in an atmospheric environment for more than one month to diffuse gas. At least five bars for each specimen under the same conditions were used for the testing, and the average values are shown with standard deviations.

3. RESULTS AND DISCUSSION

3.1. Oscillatory shear flow properties

The rheological behavior plays an important role in the polymer foaming process. To explore the influence of MDBS on the melt strength of PP, rheological parameters, including the storage modulus (G′), loss modulus (G″), loss tangent (tan δ), and complex viscosity (η*), were investigated at 190 °C. As shown in Figure 2a, the changes in G′ as a function of frequency (ω) for neat PP and PP-0.5 are presented. Both the G′ of PP and PP-0.5 increased as the frequency increased. The G″ of PP and PP-0.5 exhibited the same trend, as shown in Figure 2b. Especially at

frequencies lower than 1 rad/sec, both the G′ and G″ of PP-0.5 were far larger than those of neat PP. It can also be noticed that the effect of MDBS was more sensitive on G′ than on G″. Moreover, the frequency dependences of both the G′ and G″ of PP-0.5 became weaker. Thus, large-scale polymer relaxations in the composites were restrained as a result of the added sorbitol gelling agent. This result could be attributed to the in situ formation of the self-assembled ramified nanofibrils of MDBS, which would restrain the long-range motion of the PP chains and improve the viscoelastic properties of PP [4,56]. Figure 2c shows the frequency dependence of the loss tangent (tan δ = G″/G′) of PP and the PP-0.5 composite at 190 °C. The tan δ of neat PP monotonically increased with a decreasing frequency, while the P-0.5 exhibited some difference: the tan δ of PP-0.5 composite decreased with an increasing frequency in the high-frequency region. This result indicated that the elastic response of the PP melt became more significant in the high-frequency region [57,58]. Additionally, the change in tan δ against frequency became nearly flat at low frequencies. This phenomenon could be understood as a result of enhanced molecular entanglement, attributed to the added MDBS [6,57]. The high shear stress in neat PP by an increasing frequency led to breaking the molecular entanglements of PP, while PP-0.5 with the addition of a small amount of MDBS could effectively resist the influence of high shear stress, exhibiting solid-like behavior, which greatly reinforced the melt.

The complex viscosity, η*, is also a critical parameter influencing the foaming behavior. A high viscosity produces high strain-induced stress that increases the driving forces of cell nucleation and suppresses cell coalescence and collapse. Figure 2d shows the η* values of PP and PP-0.5. The addition of 0.5 wt% MDBS to PP increased η*, especially at low frequencies. This result indicated that MDBS could reinforce the PP melt. This phenomenon could be attributed to the formation of the self-assembled ramified nanofibrils of MDBS, which increased the molecular

entanglements of PP. These changes in the rheology of PP possibly benefited the subsequent foaming process [4,6].

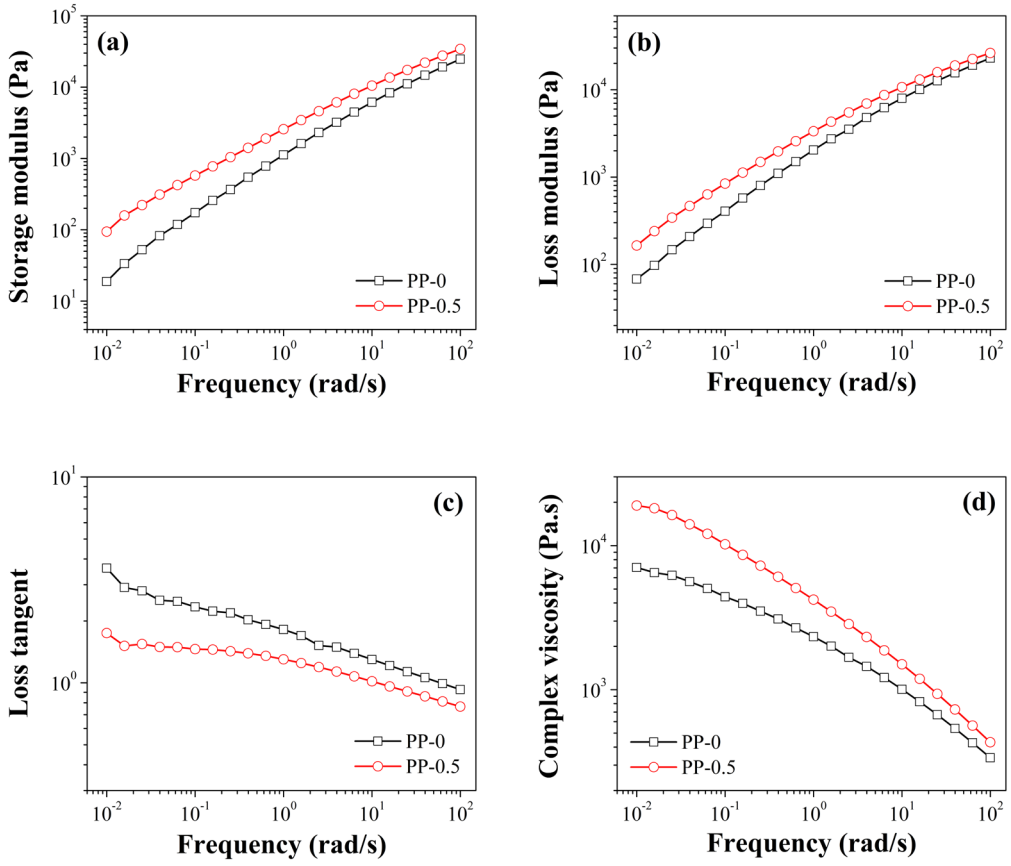

Figure 2. Change in the (a) storage modulus, G'; (b) loss modulus, G''; (c) loss tangent, $tan\ \delta$; and (d) complex viscosity, $\eta*$, as a function of frequency for the neat PP and PP-0.5 composite.

3.2. Thermal properties

It is also well known that the crystallization behavior shows a significant influence on the foaming behavior of semicrystalline polymers [7,59–61]. To clarify the foaming behavior, it is necessary to study the crystal nucleating ability of MDBS on the cooling process of PP. As shown in the Supporting Information (Figure S1), PP-0.5 samples had many more smaller crystals than the PP-0 samples due to the presence of MDBS acting as a crystal nucleating agent. The reduced

crystal size of PP due to the presence of nanoparticles has also been reported by others [5]. To further study the effect of MDBS on the crystal nucleating ability, the nonisothermal cooling thermograms of the neat PP and PP-0.5 composite at a cooling rate in the range from −2 to −20 °C/min were investigated. The nonisothermal crystallization cooling process was studied here since the crystallization behavior of the polymer occurred nonisothermally in the foam injection molding process [62−64]. Figure 3 displays the cooling curves of PP-0 and PP-0.5 at different cooling rates. Generally, the presence of MDBS effectively contributed to the shift in the crystallization peak temperature (T_c) of PP to a higher temperature than that of neat PP [55]. Table 2 lists the crystallization parameters of the neat PP and PP-0.5 composite obtained from the thermal analysis. As presented in Table 2, the T_c of the neat PP sample at −2, −5, −10, and −20 °C/min was 128.4, 124.2, 121.2, and 118.3 °C, respectively, while the corresponding T_c of the PP-0.5 composite at −2, −5, −10, and −20 °C/min was 132.1, 129.1, 126.9, and 124.1 °C, respectively. Moreover, the melting peak temperature (T_p) of PP-0.5 was higher than that of neat PP at any cooling rate. These increases in the T_c and T_p of the PP-0.5 sample were ascribed to the fact that MDBS played a role as the crystal nucleating agent and promoted its crystallization [41,55]. As a result, the increase in crystallization temperature and the melting temperature meant that the molecular chain mobility was enhanced [65,66]. These results would be beneficial for the following foaming process.

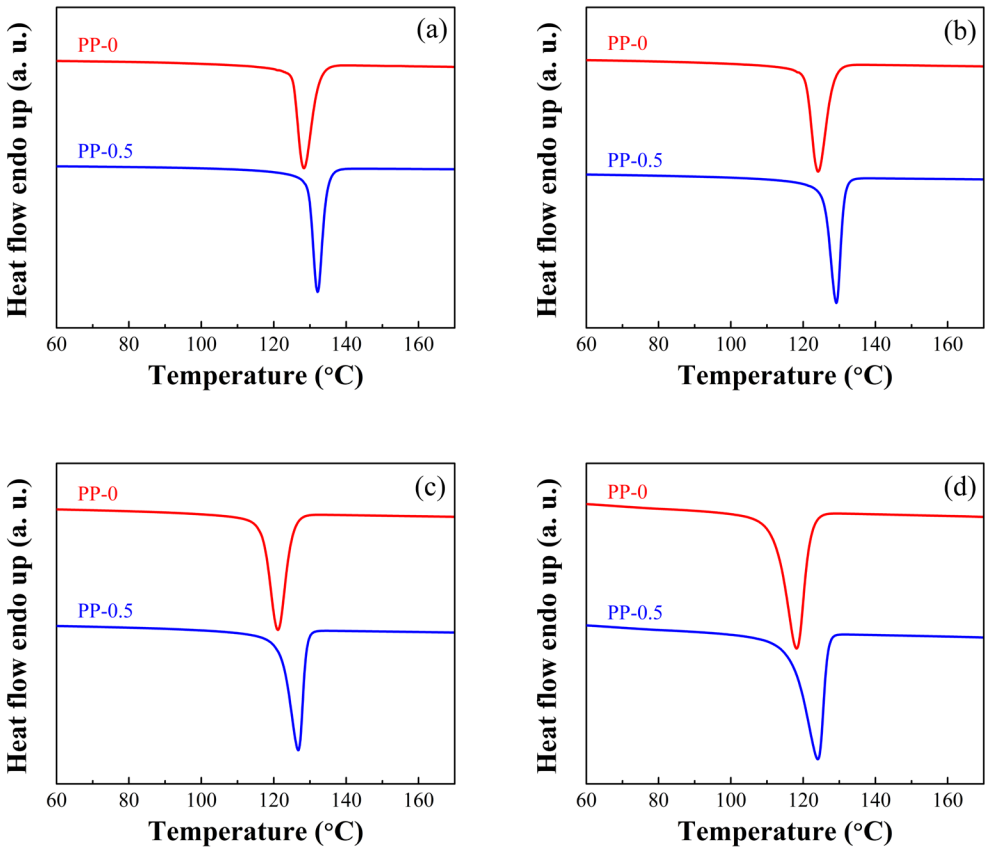

Figure 3. DSC thermograms of the nonisothermal crystallization of PP and the PP-0.5 composite at designated cooling rates of (a) 2, (b) 5, (c) 10, and (d) 20 °C/min.

The corresponding crystallinity (X_c) values of the PP-0 and PP-0.5 specimens were then calculated, and the results are summarized in Table 2. Compared with neat PP, the degree of crystallization of PP with MDBS was slightly decreased. This result indicated that the addition of MDBS, together with the coexistence of the long-chain branch structure, hindered the mobility of the molecular chain, resulting in a relatively low crystallinity [55,60]. It was assumed that the MDBS in PP-0.5 led to an increase in the density of nuclei in the crystal nucleating stage. In contrast, MDBS suppressed or disrupted the chain packing in the growing crystallites, which led to impeded crystal growth. Additionally, the long-chain branch structure could also act as heterogeneous crystal nucleation sites; thus, the increased number of crystals would further hinder

crystal growth. Hence, to a certain extent, the movement of PP chains was suppressed due to the presence of MDBS nanofibrils, leading to a decrease in the degree of crystallinity [9].

Table 2 Nonisothermal crystallization parameters of neat PP and its MD composite.

Sample	ϕ (°C/min)	T_c (°C)	T_m (°C)	ΔH_m (J/g)	Xc (%)
PP	2	128.4	156.9	94.05	45.43
	5	124.2	155.6	90.74	43.84
	10	121.2	155.1	88.49	42.75
	20	118.3	154.6	87.21	42.13
PP-0.5	2	132.1	157.7	91.05	43.99
	5	129.1	157.0	87.25	42.15
	10	126.9	156.5	84.70	40.92
	20	124.1	156.1	82.87	40.03

3.3. Effect of nucleating agents on cellular structures

In general, foams prepared via the foam injection molding technique consist of a cellular core layer and two solid skin layers [13,14, 54]. Herein, we mainly studied the difference in the cellular structures found in the core layer of the foamed specimens. Figure 4 shows the cellular structures of a core layer fabricated using low-pressure CO_2 as a foaming agent at various foaming temperatures. Following previous works, the cellular structures were analyzed in the center region taken from the view perpendicular to the core-back direction [19,55]. As shown in Figure 4, a nonuniform cellular structure with large cells was found in the neat PP foams, which was attributed to the relatively weak melt elasticity and low crystallization rate of neat PP [4,55]. Additionally, it should be noted that the neat PP used here was a type of long-chain branched PP. The poor foaming ability of this long-chain branched PP was also ascribed to the relatively low content of the physical blowing agent since the gas pressure was as low as 5 MPa in the RIC-FIM process. More efforts

should be applied to produce foams with a uniform and fine cellular structure in the RIC-FIM process. Moreover, the influence of the foaming temperature on the cellular structure of neat PP foams was not significant, which was consistent with previous findings [4,55]. In contrast, tuning the foaming temperature could improve the cell structure of the PP-0.5 composite foams. With MDBS in the PP-0.5 composite, a significant change in the cellular structure was observed by tuning the foaming temperatures from 97 to 86 °C, which was closely related to the increase in the melt strength when the foaming temperature decreased. Figure 4c′ shows that the finest cell size of the PP-0.5 foams was obtained at the lowest foaming temperature of 86 °C. Generally, the enhancement in the melt strength led to the prevention of cell wall opening and a decrease in cell collapse. In addition, the addition of MDBS improved the cell nucleation ability of PP and resulted in an increase in cell density and a reduction in cell size [4,55].

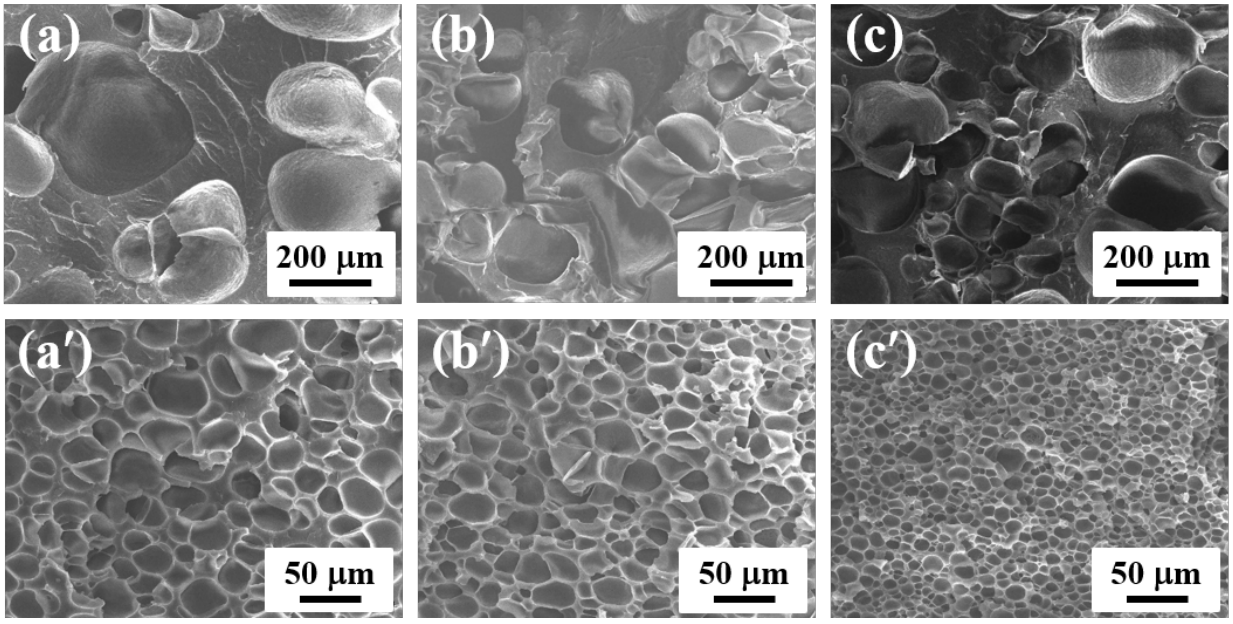

Figure 4. SEM micrographs of the neat PP foams (a–c) and PP-0.5 composite foams (a′–c′) fabricated at foaming temperatures of (a, a′) 97, (b, b′) 91, and (c, c′) 86 °C. All SEM images were taken from views perpendicular to the core-back direction.

Figure 5 summarizes the cell density and the average cell diameter of neat PP and PP-0.5 composite foams. As shown in Figure 5a, the cell density of both PP and PP-0.5 composite foams increased with a decreasing foaming temperature. This change became more obvious in the presence of MDBS in PP. Specifically, the cell density of the PP-0.5 composite foams was significantly enhanced from 6.3×10^7 to 1.3×10^9 cells/cm^3 by reducing the foaming temperature from 97 to 86 °C, achieving a nearly 20-fold increase. However, with the temperature reduction, there was only a 5-fold increase in the cell density of the neat PP foams. This difference was ascribed mainly to the increase in melt strength and viscosity as well as the enhancement in cell nucleation due to the presence of MDBS [4,55]. The improvement of the cell structure with the decrease in foaming temperature was also related to the alteration of the crystal morphology and crystallinity [6,41].

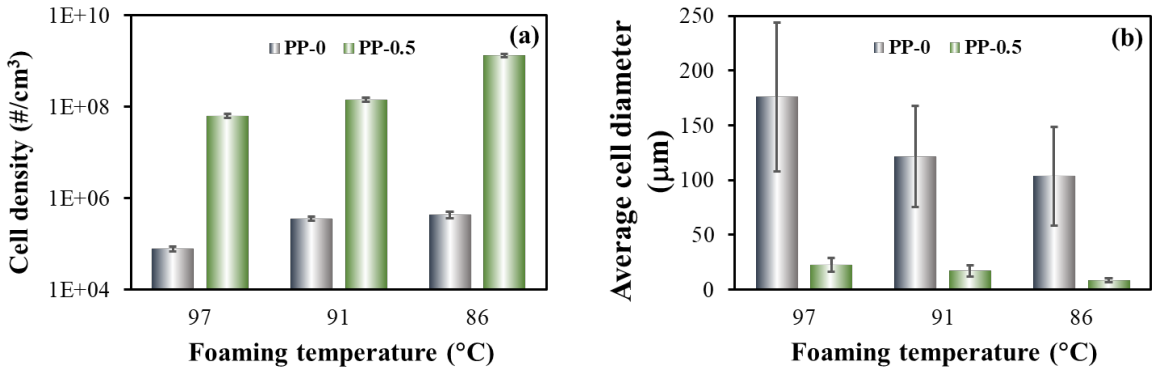

Figure 5. Change in the (a) cell density and (b) average cell diameter of the PP and PP-0.5 composite foams as a function of foaming temperature.

Figure 5b shows the changes in the cell diameters of both the PP and PP-0.5 foams against the foaming temperature. The smallest cell diameter of the PP-0.5 foams was approximately 8.4

μm in the presence of MDBS, which was achieved at 86 °C. In contrast, the average cell diameter of the neat PP foams was approximately 103.8 μm, which was much larger than that of the PP-0.5 foams. The decrease in foaming temperature would not only promote crystallization but also increase the melt strength of PP, which led to an increase in cell nucleation, a suppression of cell growth, and the eventual production of foams with much smaller cell sizes [5,48]. Thus, the optimum cellular structure of the PP-0.5 foams was achieved with the combination of an MDBS addition and the optimization of the foaming temperature, producing the finest cell structure with a cell density on the order of 10^9 cells/cm^3 and a cell diameter of less than 10.0 μm. These results demonstrated that PP foams with a well-defined cellular structure could be achieved by the addition of MDBS in the RIC-FIM process.

3.4. Mechanical performance of the injection-molded PP foams

To evaluate the effect of the fine cellular structure on the mechanical performance of both the neat PP and PP-0.5 foams, foams were prepared at various foaming temperatures and tensile tests. Figure 6 shows the stress-strain curves and tensile toughness of both the neat PP and PP-0.5 foams. As shown in Figure 6a, the neat PP foams exhibited plastic deformation before breakage and typical ductile fracture. The PP-0.5 composite foams exhibited a similar stress-strain relationship, which was breaking behavior with evident yielding and necking.

The corresponding tensile toughness obtained with the area under the stress-strain curves, which is an important index of tensile ductility, is illustrated in Figure 6b. The ductility of the PP-0.5 composite foams increased to much higher levels (by 298.1%, 447.8% and 1004.9%) than the neat PP foam by adjusting the foaming temperature from 97 to 86 °C. After the introduction of MDBS, the PP composite foams tended to become more flexible and deformable. The excellent

ductility of PP-0.5 composite foams mainly resulted from the significantly improved cellular structure and the small crystals due to the nucleating effect of MDBS [4,55]. This structure led to a sharp increase in the tensile toughness of the PP foams. In particular, the foams prepared at a foaming temperature of 86 °C, which had a high cell density and a small cell diameter, led to the cell walls of the PP-0.5 foam becoming thinner and the adjacent cells becoming much closer. As a result, it was helpful to increase the ductility of the foams because the cell walls were more easily deformed, which was consistent with previous results [5,11,55].

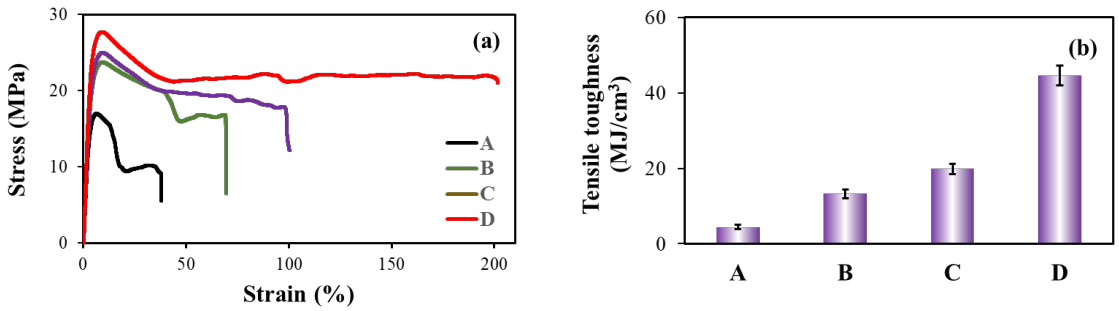

Figure 6. Mechanical properties of the (A) PP foam and PP-0.5 composite foams prepared at foaming temperatures of (B) 97, (C) 91, and (D) 86 °C. (a) Typical specific stress-strain curves. (b) Corresponding tensile toughness obtained with the area under the stress-strain curves.

Figure 7 shows the tensile strength and Young's modulus of both foams. As shown in Figure 7a, compared with the neat PP foams, the composite foams showed a notable increase in tensile strength: the tensile strength of the PP-0.5 foams prepared at foaming temperatures of 97, 91 and 86 °C were increased by 138.2%, 147.2%, and 155.9% of those of the neat PP foams, respectively. The Young's modulus of PP-0.5 foams showed a similar trend where the modulus increased as the foaming temperature decreased. This result demonstrated that incorporating the sorbitol gelling agent MDBS was very effective in enhancing both the strength and rigidity of the PP foams, which could be ascribed to improving the transfer of applied stress [67,68]. The PP-0.5 foam prepared at

the lowest foaming temperature of 86 °C showed the optimum tensile strength and rigidity. The fine and uniform cellular structure of the PP-0.5 composite foams could effectively reduce the stress concentration during the tensile measurements. Namely, crack generation and propagation were avoided, which resulted in the improved mechanical properties of the foams. These results clearly showed that MDBS could decrease the cell size and produce PP foams with desirable toughness, ductility and strength [5,69,70]. These results were very much similar to previous studies of polymer nanocomposites, where the added nanoparticles could improve the tensile properties of foams [71,72]. In summary, this work provides a promising strategy for producing lightweight microcellular injection-molded PP foams with excellent mechanical properties.

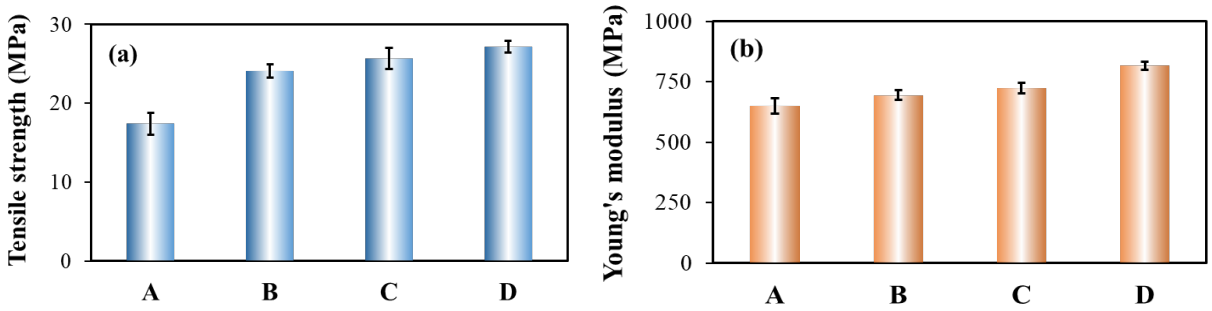

Figure 7. Details of the mechanical properties of the (A) PP foam and PP/MD composite foams prepared at foaming temperatures of (B) 97, (C) 91, and (D) 86 °C: (a) Tensile strength and (b) Young's modulus.

4. CONCLUSIONS

In this study, we prepared high-performance PP foams in the presence of a sorbitol gelling agent, MDBS, using the newly developed low-pressure FIM with low-pressure CO_2 as the foaming agent. The following conclusions were drawn.

(1) The rheological analysis revealed that the addition of the sorbitol gelling agent MDBS

could significantly improve the viscoelasticity and melt strength of PP. The DSC results showed that MDBS with only 0.5 wt% content could promote the crystallization behavior of PP.

(2) Owing to the enhanced viscoelastic properties and crystallization behavior, the addition of MDBS led to a four orders of magnitude increase in the cell density of PP foams together with a notable reduction in the cell size to approximately 8.4 μm.

(3) Remarkably, the tensile toughness and tensile strength of the PP composite foam were enhanced by 1004.9% and 155.9%, respectively. Hence, lightweight and strong PP foams with high ductility were obtained by the scalable novel RIC-FIM technique, opening up its potential application in many areas, such as automotive, construction and electrical components.

AUTHOR INFORMATION

Corresponding Author

*E-mail: wanglong@nimte.ac.cn (Long Wang); wgzheng@nimte.ac.cn (Wenge Zheng)

Address: 1219 Zhongguan West Road, Zhenhai District, Ningbo, Zhejiang, 315201 P.R. China

*E-mail: oshima@cheme.kyoto-u.ac.jp (Masahiro Ohshima).

Address: A4 Building, Kyoto Univ. Katsura Campus, Nishikyo-ku, Kyoto 615-8510, Japan

Author Contributions

This manuscript was written with contributions from all authors. All authors have given approval of the final version of this manuscript.

Notes

The authors declare no competing financial interests.

ACKNOWLEDGMENTS

This work was financially supported by the National Natural Science Foundation of China (52003280), Natural Science Foundation of Ningbo (2019A610143), Chinese Academy of Sciences Pioneer Hundred Talents Program, S&T Innovation 2025 Major Special Program of Ningbo (2018B10054), and Zhejiang Provincial Natural Science Foundation of China (LY17E030010).

REFERENCES

[1] E. Di Maio, E. Kiran, Foaming of polymers with supercritical fluids and perspectives on the current knowledge gaps and challenges, J. Supercrit. Fluid. 134 (2018) 157–166.

[2] R. Dugad, G. Radhakrishna, A. Gandhi, Recent advancements in manufacturing technologies of microcellular polymers: a review, J.Polym. Res. 27(7) (2020) 1−23.

[3] J.Y Xu, Microcellular injection molding. John Wiley and Sons Ltd.: New York. 9 (2011).

[4] L. Wang, S. Ishihara, M. Ando, A. Minato, Y. Hikima, M. Ohshima, Fabrication of high expansion microcellular injection-molded polypropylene foams by adding long-chain branches, Ind. Eng. Chem. Res. 55(46) (2016) 11970−11982.

[5] G.L. Wang, G.Q. Zhao, L. Zhang, Y. Mu, C.B. Park, Lightweight and tough nanocellular PP/PTFE nanocomposite foams with defect-free surfaces obtained using in situ nanofibrillation and nanocellular injection molding, Chem. Eng. J. 350 (2018) 1−11.

[6] L. Wang, M. Ando, M. Kubota, S. Ishihara, Y. Hikima, M. Ohshima, T. Sekiguchi, A. Sato, H. Yano, Effects of hydrophobic-modified cellulose nanofibers (CNFs) on cell morphology and mechanical properties of high void fraction polypropylene nanocomposite foams, Compos. Part A. 98 (2017) 166−173.

[7] L. Wang, S. Ishihara, Y. Hikima, M. Ohshima, T. Sekiguchi, A. Sato, H. Yano, Unprecedented

development of ultrahigh expansion injection-molded polypropylene foams by introducing hydrophobic-modified cellulose nanofibers, ACS Appl. Mater. Interfaces. 9(11) (2017) 9250−9254.

[8] A. Ameli, M. Nofar, C.B. Park, P. Poetschke, G. Rizvi, Polypropylene/carbon nanotube nano/microcellular structures with high dielectric permittivity, low dielectric loss, and low percolation threshold, Carbon. 71 (2014) 206−217.

[9] J. Zhao, Q. Zhao, C. Wang, B. Guo, C.B. Park, G. Wang, High thermal insulation and compressive strength polypropylene foams fabricated by high-pressure foam injection molding and mold opening of nano-fibrillar composites, Mater. Des. 131 (2017) 1−11.

[10] J. Peng, P.J. Walsh, R.C. Sabo, L.-S. Turng, C.M. Clemons, Water-assisted compounding of cellulose nanocrystals into polyamide 6 for use as a nucleating agent for microcellular foaming, Polymer. 84 (2016) 158−166.

[11] G.L. Wang, L. Wang, L.H. Mark, V. Shaayegan, G.Z. Wang, H.P. Li, G.Q. Zhao, C.B. Park, Ultralow-threshold and lightweight biodegradable porous PLA/MWCNT with segregated conductive networks for high-performance thermal insulation and electromagnetic interference shielding applications, ACS Appl. Mater. Interfaces. 10(1) (2018) 1195−1203.

[12] X. Sun, H. Kharbas, J. Peng, L.-S. Turng, A novel method of producing lightweight microcellular injection molded parts with improved ductility and toughness, Polymer. 56 (2015) 102−110.

[13] D. Jahani, A. Ameli, M. Saniei, W. Ding, C.B. Park, H.E. Naguib, Characterization of the structure, acoustic property, thermal conductivity, and mechanical property of highly expanded open-cell polycarbonate foams, Macromol. Mater. Eng. 300(1) (2015) 48−56.

[14] A. Ameli, D. Jahani, M. Nofar, P.U. Jung, C.B. Park, Development of high void fraction

polylactide composite foams using injection molding: Mechanical and thermal insulation properties, Compos. Sci. Technol. 90 (2014) 88−95.

[15] L. Wang, A. Yusa, Yamamoto, H. Goto, H. Uezono, F. Asaoka, Y. Hikima, S. Ishihara, M. Ohshima, A new foam injection molding technology-use non-supercritical fluids as physical blowing agents, 32nd International Conference of the Polymer Processing Society (PPS-32), S05-333, Lyon, France. (2016).

[16] A. Yusa, S. Yamamoto, H. Goto, H. Uezono, F. Asaoka, L. Wang, M. Ando, S. Ishihara, M. Ohshima, A new microcellular foam injection-molding technology using non-supercritical fluid physical blowing agents, Polym. Eng. Sci. 57(1) (2017) 105−113.

[17] L. Wang, Y. Hikima, M. Ohshima, A. Yusa, S. Yamamoto, H. Goto, Development of a simplified foam injection molding technique and its application to the production of high void fraction polypropylene foams, Ind. Eng. Chem. Res. 56(46) (2017) 13734−13742.

[18] L. Wang, Y. Wakatsuki, Y. Hikima, M. Ohshima, A. Yusa, H. Uezono, A. Naitou, Preparation of microcellular injection-molded foams using different types of low-pressure gases via a new foam injection molding technology, Ind. Eng. Chem. Res. 58(38) (2019) 17824−17832.

[19] L. Wang, Y. Hikima, M. Ohshima, A. Yusa, S. Yamamoto, H. Goto, Unusual fabrication of lightweight injection-molded polypropylene foams by using air as the novel foaming agent, Ind. Eng. Chem. Res. 57(10) (2018) 3800−3804.

[20] J. Sun, J. Zhuang, Y. Liu, H. Xu, J. Horne, E. K. Wujcik, H. Liu, J. E. Ryu, D. Wu， Z. Guo Development and application of hot embossing in polymer processing: A review, ES. Mater. Manuf. 6 (2019) 3−17.

[21] D. Zhang, J. Sun, L. J. Lee, J. M. Castro, Overview of ultrasonic assisted manufacturing multifunctional carbon nanotube nanopaper based polymer nanocomposites, Eng. Sci. 10

(2020) 35−50.

[22] Q. Ren, J. Wang, W. Zhai, R.E. Lee, Fundamental influences of induced crystallization and phase separation on the foaming behavior of poly(lactic acid)/polyethylene glycol blends blown with compressed CO_2, Ind. Eng. Chem. Res. 55(49) (2016) 12557−12568.

[23] Q. Ren, J.J. Wang, W.T. Zhai, S.P. Su, Solid State Foaming of poly(lactic acid) blown with compressed CO_2: Influences of long chain branching and induced crystallization on foam expansion and cell morphology, Ind. Eng. Chem. Res. 52(37) (2013) 13411−13421.

[24] S. Iannace, C.B. Park, Biofoams: science and applications of bio-based cellular and porous materials, CRC Press, (2015).

[25] J. Gong, G.Q. Zhao, G.L. Wang, L. Zhang, B. Li, Fabrication of macroporous carbon monoliths with controllable structure via supercritical CO_2 foaming of polyacrylonitrile, J. CO_2 Util. 33 (2019) 330−340.

[26] P. Huang, F. Wu, B. Shen, H. Zheng, Q. Ren, H. Luo, W. Zheng, Biomimetic porous polypropylene foams with special wettability properties, Compos. Part B-Eng. (2020) 107927.

[27] A. Rizvi, A. Tabatabaei, M.R. Barzegari, S.H. Mahmood, C.B. Park, In situ fibrillation of CO_2-philic polymers: Sustainable route to polymer foams in a continuous process, Polymer. 54(17) (2013) 4645−4652.

[28] L. Wang, D. Wan, J. Qiu, T. Tang, Effects of long chain branches on the crystallization and foaming behaviors of polypropylene-g-poly(ethylene-co-1-butene) graft copolymers with well-defined molecular structures, Polymer. 53(21) (2012) 4737−4757.

[29] S. Lee, L. Zhu, J. Maia, The effect of strain-hardening on the morphology and mechanical and dielectric properties of multi-layered PP foam/PP film, Polymer. 70 (2015) 173−182.

[30] P. Spitael, C.W. Macosko, Strain hardening in polypropylenes and its role in extrusion foaming,

Polym. Eng. Sci. 44(11) (2004) 2090−2100.

[31] W. Zhai, T. Kuboki, L. Wang, C.B. Park, E.K. Lee, H.E. Naguib, Cell structure evolution and the crystallization behavior of polypropylene/clay nanocomposites foams blown in continuous extrusion, Ind. Eng. Chem. Res. 49(20) (2010) 9834−9845.

[32] M. Okamoto, P.H. Nam, P. Maiti, T. Kotaka, T. Nakayama, M. Takada, M. Ohshima, A. Usuki, N. Hasegawa, H. Okamoto, Biaxial flow-induced alignment of silicate layers in polypropylene/clay nanocomposite foam, Nano. Lett. 1(9) (2001) 503−505.

[33] P.H. Nam, P. Maiti, M. Okamoto, T. Kotaka, T. Nakayama, M. Takada, M. Ohshima, A. Usuki, N. Hasegawa, H. Okamoto, Foam processing and cellular structure of polypropylene/clay nanocomposites, Polym. Eng. Sci. 42(9) (2002) 1907−1918.

[34] W.G. Zheng, Y.H. Lee, C.B. Park, Use of nanoparticles for improving the foaming behaviors of linear PP, J. Appl. Polym. Sci. 117(5) (2010) 2972−2979.

[35] P.K. Hou, R. Li, Q.F. Li, N. Lu, K.J. Wang, M.L. Liu, X. Cheng, S. Shah, Novel superhydrophobic cement-based materials achieved by construction of hierarchical surface structure with FAS/SiO_2 hybrid nanocomposites, ES. Mater. Manuf. 1 (2018), 57−66.

[36] H.B Gu, X.J. Xu, H.Y. Zhang, C.B. Liang, H. Lou, C. Ma, Y.J. Li, Z.H. Guo, J.W. Gu, Chitosan-coated-magnetite with covalently grafted polystyrene based carbon nanocomposites for hexavalent chromium adsorption, Eng. Sci. 1 (2018) 46−54.

[37] R. Das, S. Vupputuri, Q. Hu, Y. Chen, H. Colorado, Z.H. Guo, Z. Wang, Synthesis and characterization of antiflammable vinyl ester resin nanocomposites with surface functionalized nanotitania, ES. Mater. Manuf. 8 (2020) 46−53.

[38] Q. Wang, J. Zhang, Z. Zhang, Y. Hao, K. Bi, Enhanced dielectric properties and energy storage density of PVDF nanocomposites by co-loading of $BaTiO_3$ and $CoFe_2O_4$ nanoparticles, Adv.

Compos. Hybr. Mater. 3(1) (2020) 58−65.

[39] J. Wang, Z.C. Shi, X. Wang, X.M. Mai, R.H. Fan, H. Liu, X.J. Wang, Z.H. Guo, Enhancing dielectric performance of poly(vinylidene fluoride) nanocomposites via controlled distribution of carbon nanotubes and barium titanate nanoparticle, Eng. Sci. 4 (2018) 79−86.

[40] M. Antunes, M. Mudarra, J. Ignacio Velasco, Broad-band electrical conductivity of carbon nanofibre-reinforced polypropylene foams, Carbon. 49(2) (2011) 708−717.

[41] L. Wang, Y. Hikima, M. Ohshima, T. Sekiguchi, H. Yano, Evolution of cellular morphologies and crystalline structures in high-expansion isotactic polypropylene/cellulose nanofiber nanocomposite foams, RSC Adv. 8(28) (2018) 15405−15416.

[42] L. Shi, G. Song, P. Li, X. Li, D. Pan, Y. Huang, L. Ma, Z. Guo, Enhancing interfacial performance of epoxy resin composites via in-situ nucleophilic addition polymerization modification of carbon fibers with hyperbranched polyimidazole, Compos. Sci. Technol. 201 (2021) 108522 (1−8).

[43] P. Feng, L. Ma, G. Wu, X. Li, M. Zhao, L. Shi, M. Wang, X. Wang, G. Song, Establishment of multistage gradient modulus intermediate layer between fiber and matrix via designing double "rigid-flexible" structure to improve interfacial and mechanical properties of carbon fiber/resin composites, Compos. Sci. Technol. 200 (2020) 108336 (1−8).

[44] L.F. Lyu, J.R. Liu, H. Liu, C.T Liu, Y. Lu, K. Sun, R.H. Fan, N. Wang, N. Lu, Z.H. Guo, E. K. Wujcik, An overview of electrically conductive polymer nanocomposites toward electromagnetic interference shielding, Eng. Sci. 2 (2018) 26−42.

[45] A.A.B. Omran, A.A.B.A. Mohammed, S.M. Sapuan, R.A. Ilyas, M.R.M. Asyraf, S.S. Rahimian Koloor, M. Petru, Micro- and nanocellulose in polymer composite materials: A Review, Polymers. 13(2) (2021) 2311(1−35).

[46] N.H. Sari, C.I. Pruncu, S.M. Sapuan, R.A. Ilyas, A.D. Catur, S. Suteja, Y.A. Sutaryono, G. Pullen, The effect of water immersion and fibre content on properties of corn husk fibres reinforced thermoset polyester composite, Polym. Test. 91 (2020) 106751(1−8).

[47] X.R. Yan, J.J. Liu, M.A. Khan, S. Sheriff, S. Vupputuri, R. Das, L. Sun, D. P. Young, Z.H. Guo, Efficient solvent-free microwave irradiation synthesis of highly conductive polypropylene nanocomposites with lowly loaded carbon nanotubes, ES. Mater. Manuf. 9 (2020) 21−33.

[48] A. Rizvi, R.K. Chu, J.H. Lee, C.B. Park, Superhydrophobic and oleophilic open-cell foams from fibrillar blends of polypropylene and polytetrafluoroethylene, ACS Appl. Mater. Interface. 6(23) (2014) 21131−21140.

[49] S. Ishihara, Y. Hikima, M. Ohshima, Preparation of open microcellular polylactic acid foams with a microfibrillar additive using coreback foam injection molding processes, J. Cell. Plasti. 54(4) (2018) 765−784.

[50] M. Kristiansen, M. Werner, T. Tervoort, P. Smith, M. Blomenhofer, H.-W. Schmidt, The binary system isotactic polypropylene/bis (3, 4-dimethylbenzylidene) sorbitol: phase behavior, nucleation, and optical properties, Macromolecules. 36(14) (2003) 5150−5156.

[51] J. Lipp, M. Shuster, G. Feldman, Y. Cohen, Oriented crystallization in polypropylene fibers induced by a sorbitol-based nucleator, Macromolecules. 41(1) (2008) 136−140.

[52] K. Sreenivas, R. Basargekar, G. Kumaraswamy, Phase separation of DMDBS from PP: effect of polymer molecular weight and tacticity, Macromolecules. 44(7) (2011) 2358−2364.

[53] J. Lipp, M. Shuster, A.E. Terry, Y. Cohen, Fibril formation of 1, 3: 2, 4-di (3, 4-dimethylbenzylidene) sorbitol in a polypropylene melt, Langmuir. 22(14) (2006) 6398−6402.

[54] R. Miyamoto, S. Yasuhara, H. Shikuma, M. Ohshima, Preparation of micro/nanocellular

polypropylene foam with crystal nucleating agents, Polym. Eng. Sci. 54(9) (2014) 2075−2085.

[55] L. Wang, Y. Hikima, S. Ishihara, M. Ohshima, Fabrication of lightweight microcellular foams in injection-molded polypropylene using the synergy of long-chain branches and crystal nucleating agents, Polymer. 128 (2017) 119−127.

[56] P. Pötschke, T.D. Fornes, D.R. Paul, Rheological behavior of multiwalled carbon nanotube/polycarbonate composites, Polymer. 43(11) (2002) 3247−3255.

[57] P. Pötschke, M. Abdel-Goad, I. Alig, S. Dudkin, D. Lellinger, Rheological and dielectrical characterization of melt mixed polycarbonate-multiwalled carbon nanotube composites, Polymer. 45 (2004) 8863−8870.

[58] Y.T. Sung, M.S. Han, K.H. Song, J.W. Jung, H.S. Lee, C.K. Kum, J. Joo, W.N. Kim, Rheological and electrical properties of polycarbonate/multi-walled carbon nanotube composites, Polymer. 47(12) (2006) 4434−4439.

[59] M. Nofar, C.B. Park, Poly (lactic acid) foaming, Prog. Polym. Sci. 39 (2014) 1721−1741.

[60] A.R. Kakroodi, Y. Kazemi, W.D. Ding, A. Ameli, C.B. Park, Poly(lactic acid)-based in situ microfibrillar composites with enhanced crystallization kinetics, mechanical properties, rheological behavior, and foaming ability, Biomacromolecules. 16 (2015) 3925–3935.

[61] A. Tabatabaei, C.B. Park, In-situ visualization of PLA crystallization and crystal effects on foaming in extrusion, Eur. Polym. J. 96 (2017) 505−519.

[62] E. Zhuravlev, V. Madhavi, A. Lustiger, R. Androsch, C. Schick, Crystallization of polyethylene at large undercooling, Acs. Macro. Lett. 5(3) (2016) 365−370.

[63] A.M. Rhoades, N. Wonderling, A. Gohn, J. Williams, D. Mileva, M. Gahleitner, R. Androsch, Effect of cooling rate on crystal polymorphism in beta-nucleated isotactic polypropylene as revealed by a combined WAXS/FSC analysis, Polymer. 90 (2016) 67−75.

[64] A. Toda, R. Androsch, C. Schick, Insights into polymer crystallization and melting from fast scanning chip calorimetry, Polymer. 91 (2016) 239−263.

[65] A. Tabatabaei, L.H. Mark, C.B. Park, Visualization of polypropylene crystallites formed from a stressed melt in extrusion, Polymer. 101 (2016) 48−58.

[66] A. Tabatabaei, M.R. Barzegari, L.H. Mark, C.B. Park, Visualization of polypropylene's strain-induced crystallization under the influence of supercritical CO_2 in extrusion, Polymer. 122 (2017) 312−322.

[67] M. Shimbo, I. Higashitani, Y. Miyano, Mechanism of strength improvement of foamed plastics having fine cell, J. Cell. Plast. 43(2) (2007) 157−167.

[68] H.B. Zhang, Q. Yan, W.G. Zheng, Z. He, Z.Z. Yu, Tough graphene-polymer microcellular foams for electromagnetic interference shielding, ACS Appl. Mater. Inter. 3(3) (2011) 918−924.

[69] G. Wang, G. Zhao, S. Wang, L. Zhang, C.B. Park, Injection-molded microcellular PLA/graphite nanocomposites with dramatically enhanced mechanical and electrical properties for ultra-efficient EMI shielding applications, J. Mater. Chem. C. 6(25) (2018) 6847 (1-14).

[70] G.L. Wang, J.C. Zhao, G.Z. Wang, H.B. Zhao, J. Lin, G.Q. Zhao, C.B. Park, Strong and super thermally insulating in-situ nanofibrillar PLA/PET composite foam fabricated by high-pressure microcellular injection molding, Chem. Eng. J. 390 (2020) 124520−124534.

[71]]W. Zhao, L. Chen, S. Hu, Z. Shi, X. Gao, V.V. Silberschmidt, Printed hydrogel nanocomposites: fine-tuning nanostructure for anisotropic mechanical and conductive properties, Adv. Compos. Hybr. Mater. 3(3) (2020) 315−324.

[72] P. Xu, M. Qu, Y. Ning, T. Jia, Y. Zhang, S. Wang, N. Feng, L. Wu, High performance and low floating fiber glass fiber-reinforced polypropylene composites realized by a facile coating method, Adv. Compos. Hybr. Mater. 2(2) (2019) 234−241.